Crystallization Kinetics of Isotactic Polypropylene Nucleated with Organic Dicarboxylic Acid Salts

Shicheng Zhao, Zhong Xin

State Key Laboratory of Chemical Engineering and Product Engineering, Department of School of Chemical Engineering, East China University of Science and Technology, Shanghai 200237, People's Republic of China

Received 8 February 2008; accepted 25 October 2008
DOI 10.1002/app.29689
Published online 5 February 2009 in Wiley InterScience (www.interscience.wiley.com).

ABSTRACT: Bicyclo[2.2.1]hept-5-ene-2,3-dicarboxylate salts (BCHED) were synthesized by hydrothermal method. The crystallization kinetics of isotactic polypropylene (iPP) and nucleated iPP with BCHED were investigated by differential scanning calorimeter (DSC) under isothermal and nonisothermal conditions. Isothermal crystallization kinetics was described by Avrami equation and the fold surface free energy (σ_e) of iPP was calculated by Hoffman theory. The results showed Avrami exponents of nucleated iPP become smaller, the values of $t_{1/2}$ dramatically decrease, the crystallization rate constants $Z(T)$ greatly increase and the fold surface free energy (σ_e) of iPP decrease with the addition of the nucleating agents. Under nonisothermal condition the Caze method was applied to deal with the crystallization kinetics of iPP and the crystallization active energy of iPP was determined by Kissinger method. The results showed the crystallization peak temperatures (T_{cp}) of nucleated iPP greatly increase, but Avrami exponents of iPP were slightly influenced and the crystallization active energy of iPP increases by the addition of BCHED. It can be concluded that BCHED act as nucleating agents and BCHE11 shows the best nucleating effect. © 2009 Wiley Periodicals, Inc. J Appl Polym Sci 112: 1471–1480, 2009

Key words: crystallization kinetics; nucleating agent; isotactic polypropylene; bicyclo[2.2.1]heptene dicarboxylate salts

INTRODUCTION

The crystallization of isotactic polypropylene (iPP) is generally described in terms of a crystalline nucleation and growth model, and the rate of nucleation determines the rate of overall crystallization.[1] It is assumed that nuclei form from ordered segments as a result of thermal fluctuations in the melt and then these nuclei grow by the addition of more segments until a stable crystalline structure develops. The addition of nucleating agents can accelerate the process of crystalline nucleation by providing massive foreign nucleation sites. Up to now, the use of nucleating agents in isotactic polypropylene is widespread and of great commercial importance because the control of the crystallization process allows one to modify the optical, mechanical, and processing properties of iPP.

A large number of compounds have been reported to nucleate the α-form of PP.[2–13] These nucleating agents are mainly categorized into three types by the structure: (1) sorbitol derivatives,[2–4] such as 1,3 : 2,4-dibenzylidenesorbitol (DBS, Millad 3905, Milliken Chemical and Irgaclear D, Ciba speciality Chemicals), bis(3,4-dimethybenzylidene)-sorbitol (DMDBS, Millad 3988); (2) organic phosphate derivatives,[5–12] such as sodium 2,2-methylene-bis (4,6-di-*tert*-butylphenyl) phosphate (commercial product name: ADK STAB NA-11) and aluminum salt of 2,2-methylene-bis (4,6-di-*tert*-butylphenyl) phosphate (commercial product name: ADK STAB NA-21); and (3) organic carboxylic acid salt,[12–14] such as sodium benzoate and salts of dehydroabietic acid. The effect of these nucleating agents on crystallization behavior and kinetics of iPP had been extensively investigated.[2–14] However, effects of organic dicarboxylic acid salts acting as α-nucleating agents on crystallization behavior of iPP are rarely studied.[14] It was reported that bicyclo[2.2.1]hept-5-ene-2,3-dicarboxylate salts (BCHED) are effective nucleating agents.[15] Especially, it exhibits significantly higher polymer crystallization peak temperature, shorter crystallization half-time. So far, the crystallization kinetics of iPP nucleated with the nucleators was not reported. Undoubtedly, the study of crystallization kinetics of nucleated iPP is meaningful to industry processing and application.

In this article, the effects of BCHED on the crystallization kinetics of iPP were investigated. The isothermal and nonisothermal crystallization experiments of virgin iPP and nucleated iPP were carried out by differential scanning calorimetry (DSC). Avrami equation

Correspondence to: Z. Xin (xzh@ecust.edu.cn).
Contract grant sponsor: National Natural Science Foundation of China; contract grant number: 20876042.

was used to describe the isothermal crystallization kinetics. The fold surface free energy (σ_e) of virgin iPP and nucleated iPP was calculated by Hoffman theory.[16] Caze method[17] was chosen to describe the nonisothermal crystallization kinetics since it can avoide to select the zero point of crystallization, whereas other methods such as Jeziorny method,[18] Ozawa method,[19] and Mo method[20] involve the zero point selection, which has obvious effect on the calculated results. The crystallization activation energy was evaluated by using Kissinger's method.[21]

EXPERIMENTAL

Materials

The iPP powder (T30S) used in this study was kindly provided by Jiujiang petrochemical Corp. (China). The material has a melt flow index of 3.4 g/10 min. The nucleating agents are metal salts of bicycle[2.2.1]hept-5-ene-2,3-dicarboxylate (BCHED), and their structures are shown in Scheme 1. BCHED were synthesized by hydrothermal method according to literature.[15] These nucleating agents were white powder and their melting points are above 300°C.

Sample preparation

The nucleating agents (0.2 wt %) and antioxidant (0.1 wt %) were added into the iPP powders then mixed in a high-speed mixer for 5 min. The mixture was extruded by an SJSH-30 twin-screw extruder (Nanjing Rubber and Plastics Machinery Plant Co., Ltd., China) through a strand die and palletized for DSC measurement.

Apparatus and experimental procedures

A Perkin–Elmer Diamond DSC (Perkin–Elmer Company) was used for calorimetric investigations of isothermal and nonisothermal crystallization. Calibration was performed using pure indium at a heating rate of 10 K/min. All DSC operations were carried out under a nitrogen environment. The sample weights were ~ 3 mg and all samples were heated to 473 K and hold in the molten state for 5 min to eliminate the thermal history. In isothermal crystallization experiments, the sample melts were subsequently rapidly cooled to the crystallization temperature (T_c) and maintained until the crystallization of matrix was completed. The exotherms were recorded at the selected crystallization temperature. Nonisothermal crystallization experiments were carried out by cooling samples from 473 to 323 K using different cooling rates. The exotherms were recorded with the cooling rates 5, 10, 20, 30, and 40 K/min, respectively.

Theory of crystallization

The Avrami equation[22,23] is widely used to describe the polymer isothermal crystallization.

$$X_t = 1 - \exp(-Z(T)t^n) \quad (1)$$

where, X_t is the relative crystallinity at time t, n is a constant whose value depends on the mechanism of nucleation and on the form of crystal growth, and $Z(T)$ is a constant containing the nucleation and growth parameters.

Crystallization half-time ($t_{1/2}$), defined as the time to a relative crystallinity of 50%, can be obtained as follows:

$$t_{1/2} = \left(\frac{\ln 2}{Z(T)}\right)^{1/n} \quad (2)$$

The time at maximum heat flow (t_{max}) can be calculated by the following:

$$t_{max} = [(n-1)/nZ(T)]^{1/n} \quad (3)$$

The Avrami equation has been extended by Ozawa to develop a simple method to study the

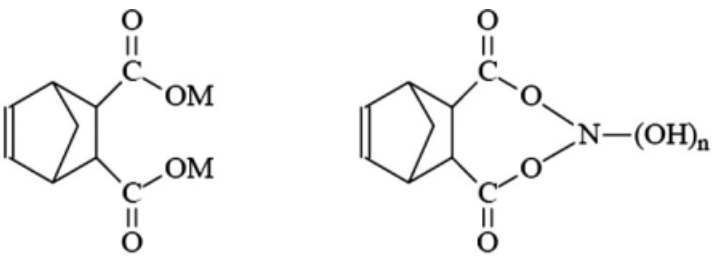

Name	BCHE03	BCHE11	BCHE19	Name	BCHE12	BCHE20	BCHE13
M	Li	Na	K	N	Mg	Ca	Al
				n	0	0	1

Scheme 1 Structure of nucleating agents in this study.

nonisothermal experiment. The general form of Ozawa theory is written as follows:

$$X_v(T) = 1 - \exp(-K_T/\Phi^m) \quad (4)$$

where, K_T is the cooling crystallization function, Φ is the cooling rate, and m is the Ozawa exponent that depends on the dimension of the crystal growth. In Ozawa method, there is a main hypothesis that n is independent of temperature and only a limited number of X_v data are available for the foregoing analysis, as the onset of crystallization varies considerably with the cooling rate.

Caze et al.[17] put forward a new method to modify Ozawa equation. It was assumed an exponential increase of K_T with T upon cooling. On the basis, the temperature at the peak and the two inflection points of the exotherm with skew Gaussian shape are linearly related to ln Φ to estimate the exponent n.

On the basis of the findings on the crystallization behavior of poly (ethylene terephthalate) and PP, Kim et al.[24] proposed the following:

$$\ln K_T = a(T - T_1) \quad (5)$$

where, a and T_1 are empirical constants. If the extreme point of the pertinent $(\partial X_v(T)/\partial T)$ curve occurs at $T = T_q$ (crystallization peak temperature), i.e., $(\partial^2 X_v(T)/\partial T^2)_{T_q} = 0$, we have the following:

$$K_T(T_q) = \Phi^n \quad (6)$$

Combining eqs. (4)–(6) yields the following:

$$\ln[-\ln(1 - X_v(T))] = a(T - T_q) \quad (7)$$

Hence, a linear plot of $\ln[-\ln(1 - X_v(T))]$ versus T would result in the constant a and the product $-aT_q$ from the gradient and intercept, respectively. At $T = T_q$, obtained from the foregoing algorithm, eqs. (6) and (7) lead to:

$$T_q = n \ln \Phi/a + T_1 \quad (8)$$

As such, parameter n can be obtained from the linear plot of T_q versus ln Φ/a in accordance with eq. (8).

RESULTS AND DISCUSSION

Isothermal crystallization

Isothermal crystallization behavior of virgin iPP and nucleated iPP are studied by DSC at various temperatures. The heat flow evolution of virgin iPP and typical representative (iPP/BCHE11) of nucleated iPP were obtained (Fig. 1) by cooling the molten polymer to the crystallization temperature and other

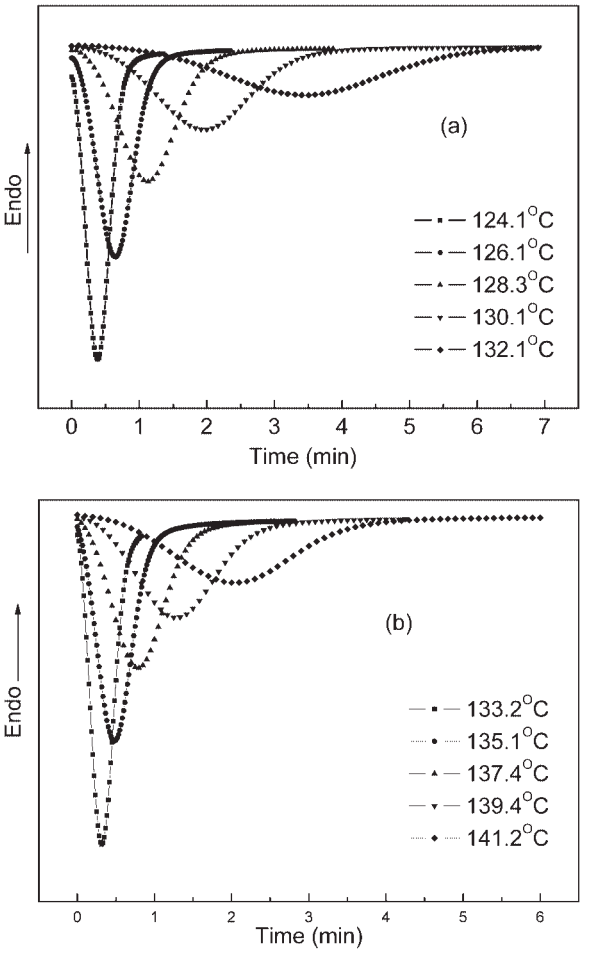

Figure 1 Heat flow curves of (a) iPP and (b) iPP/BCHE11 during isothermal crystallization.

nucleated iPP samples showed the similar results. The effects of crystallization temperature and nucleating agents on crystallization rate of iPP are clearly observed in isothermal thermograms. With the increasing of crystallization temperature, the exothermal peak in DSC curves shifts right obviously, which indicates that crystallization time prolongs and crystallization rate decreases. With the addition of BCHE11, the crystallization time of nucleated iPP obviously shorten compared with that of pure iPP, which shows that BCHE11 can greatly improve the crystallization rate due to the heterogeneous nucleation. Other nucleating agents have similar results but shows different degree in the increasing of crystallization temperature and the decreasing of crystallization time. From the heat flow evolution, the time at maximum heat flow (t_{max}) can be obtained and the results are listed in Table I.

The effect is more evident in the relative crystallinity curves obtained by integration of the exothermal peaks, which are showed in Figure 2. The relative crystallinity (X_t) is expressed as follows:

TABLE I
Isothermal Crystallization Kinetics Parameters of iPP and Nucleated iPP

Sample	T_c (°)	n	Z^t ($\min_{-n}$)	$t_{1/2}$[a] (s)	$t_{1/2}$[b] (s)	t_{max}[a] (s)	t_{max}[c] (s)	n (average)	$K_g(10^5K^2)$	σ_e, J/m^2
iPP	124.1	2.75	8.93	23	24	22	23	3.24 ± 0.36	10.00	0.166
	126.1	3.01	2.59	37	39	37	38			
	128.3	3.32	0.46	65	68	65	68			
	130.1	3.54	0.063	112	118	112	119			
	132.1	3.60	0.0077	200	209	200	212			
iPP/BCHE03	131.3	2.14	10.20	17	17	16	15	2.39 ± 0.18	7.51	0.125
	133.1	2.27	3.88	24	28	24	26			
	135.1	2.47	1.20	47	48	46	45			
	137.1	2.46	0.42	72	74	71	69			
	139.1	2.59	0.12	116	118	114	113			
iPP/BCHE11	133.2	2.55	11.27	20	20	19	19	2.68 ± 0.21	6.41	0.107
	135.1	2.42	3.51	30	31	29	29			
	137.4	2.66	1.18	49	49	47	47			
	139.4	2.86	0.30	79	80	77	79			
	141.2	2.92	0.079	123	126	122	124			
iPP/BCHE19	133.1	2.68	2.30	38	38	37	37	2.85 ± 0.15	7.33	0.122
	135.4	2.99	0.50	67	67	66	66			
	137.2	2.97	0.10	114	115	112	113			
	139.2	2.92	0.024	188	190	187	186			
	141.1	2.69	0.0082	304	312	306	301			
iPP/BCHE12	124.6	3.37	13.20	26	25	26	25	3.11 ± 0.28	9.09	0.151
	126.4	2.67	3.21	35	34	33	33			
	128.4	3.01	0.70	61	60	59	59			
	130.1	3.29	0.13	101	100	99	100			
	132.0	3.23	0.035	150	151	148	151			
iPP/BCHE20	131.4	2.51	12.34	19	19	19	18	2.76 ± 0.16	6.69	0.111
	133.3	2.79	4.29	31	31	28	30			
	135.5	2.89	1.19	50	50	46	49			
	137.5	2.72	0.35	76	77	71	75			
	139.1	2.91	0.13	107	107	101	105			
iPP/BCHE13	131.3	3.03	6.23	29	29	28	29	3.11 ± 0.11	10.74	0.175
	133.2	3.22	0.62	62	62	61	62			
	135.1	2.96	0.061	133	136	133	134			
	137.1	3.21	0.0048	280	282	283	282			
	139.1	3.15	0.00080	512	514	525	511			

[a] Determined from heat flow curves.
[b] Calculated from eq. (2).
[c] Calculated from eq. (3).

$$X_t = \frac{X_t(t)}{X_t(\infty)} = \frac{\int_0^t (dH(t)/dt)dt}{\int_0^\infty (dH(t)/dt)dt} \quad (9)$$

where, $dH(t)/dt$ represents the heat flow, $X_t(t)$ and $X_t(\infty)$ denote the absolute crystallinity at time t and at the termination of the crystallization process, respectively.

From Figure 2, the crystallization half-time ($t_{1/2}$) can be obtained and the results are listed in Table I.

The typical Avrami plots obtained at various temperatures are illustrated for virgin iPP and iPP/BCHE11 in Figure 3. There is good linearity of $\ln[-\ln(1 - X_t)]$ versus $\ln t$ in the primary stages of isothermal crystallization for pure iPP and nucleated iPP, which indicates that Avrami equation is suitable to this study. Furthermore, the agreement of the values of $t_{1/2}$ and t_{max} obtained from the experiment data and from Avrami equation also indicates the validity of the Avrami equation in this study. The Avrami exponent (n) and the rate constant ($Z(T)$) can be obtained from of the slope and intercept of these straight lines. The values of $Z(T)$ and n are listed in Table I.

From Table I, it was shown that at same crystallization temperature (for example, 133°C) the values of n for iPP containing the nucleating agents are smaller than that for pure iPP due to the heterogeneous nucleation. The values of $Z(T)$ for all nucleated iPP are larger than that of pure iPP, which further proves that the crystallization of iPP is accelerated by the nucleating agents. Compared $t_{1/2}$ and t_{max} of nucleated iPP and pure iPP, it is found that different metal salts of bicyclo[2.2.1]hept-5-ene-2,3-dicarboxylate show different nucleation efficiency even if the valence of metal is the same. Among them, BCHE11 shows the best nucleating effect. And the order is BCHE11, BCHE03, BCHE20, BCHE19, BCHE13, and BCHE12. For the difference of nucleating ability, this

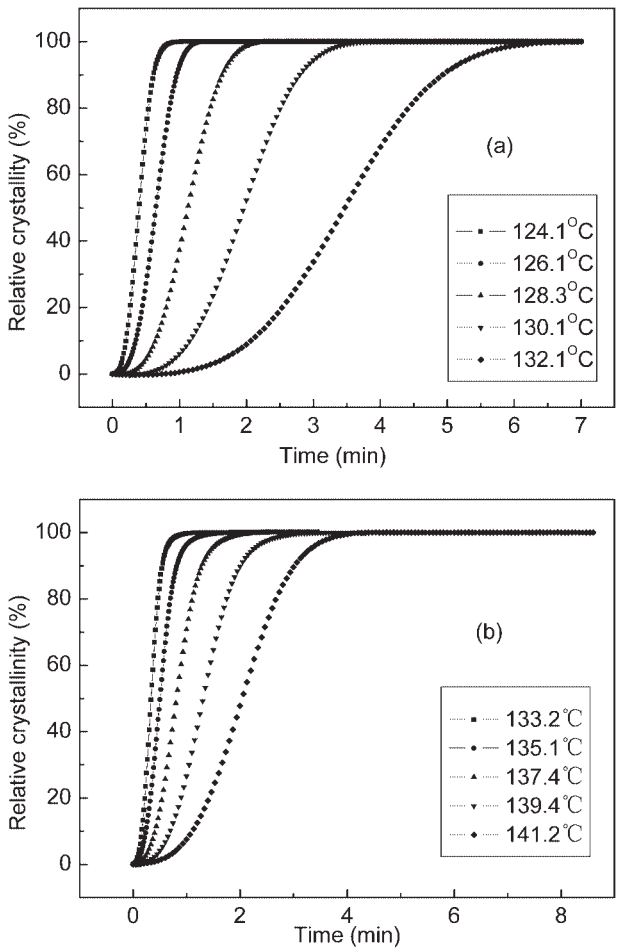

Figure 2 Relative crystallinity versus time for (a) iPP and (b) iPP/BCHE11 during isothermal crystallization.

can be ascribed to matching degree between the nucleating agents and iPP. The nucleation efficiency will be improved with the increasing matching degree. Yoshimoto et al.[8] investigate the crystallization behavior of sodium 2,2′-methylene-bis(4,6-di-*t*-butylphenylene) phosphate (NA11) on iPP and thought that effectiveness of nucleating agents was due to whether or not they cause the epitaxial crystallization by lattice matching between the nucleating agents and iPP.

According to the Hoffman theory, the growth rate of crystals (G) can be expressed as follows:[8,16]

$$G = G_0 \exp\left[-\frac{U^*}{R(T_c - T_\infty)}\right] \exp\left[-\frac{K_g}{T_c \Delta T f}\right] \qquad (10)$$

where, G_0 is a pre-exponential factor, R is the gas constant, U^* is the activation energy of polymer segments transporting to the crystal front through the subcooled melt and U^* is 6270 J/mol for iPP. T_∞ is the temperature at which all motion associated with viscous flow ceases and is taken as $T_g - 30$ K (T_g is 263 K for iPP). T_c is the crystallization temperature. ΔT is the degree of supercooling ($T_m^0 - T_c$), where T_m^0 is the equilibrium melting temperature (T_m^0 is 481 K for iPP). f is a correcting factor for temperature dependence of fusion heat and is approximated by $f = 2T_c/(T_m^0 + T_c)$, and K_g is the nucleation constant for a given growth regime.

It is assumed that the crystal growth mechanism of the polymer is a three-dimensional spherulite, and the number of nuclei in isothermal crystallization is constant, the growth rate G is reciprocally proportional to the half crystallization time ($t_{1/2}$). Then, we obtain as follows:

$$\ln(t_{1/2})^{-1} + \frac{U^*}{R(T_c - T_\infty)} = A - \frac{K_g}{T_c \Delta T f} \qquad (11)$$

Thus, the plot of $\ln(t_{1/2})^{-1} + \frac{U^*}{R(T_c - T_\infty)}$ versus $1/(-T_c \Delta T f)$ will give a straight line (Fig. 4), and K_g can be determined from the slope of the line. The results are listed in Table I.

The fold surface free energy (σ_e) can be obtained by the following equation:

$$K_g = \frac{4\sigma\sigma_e b_0 T_m^0}{k\Delta H} \qquad (12)$$

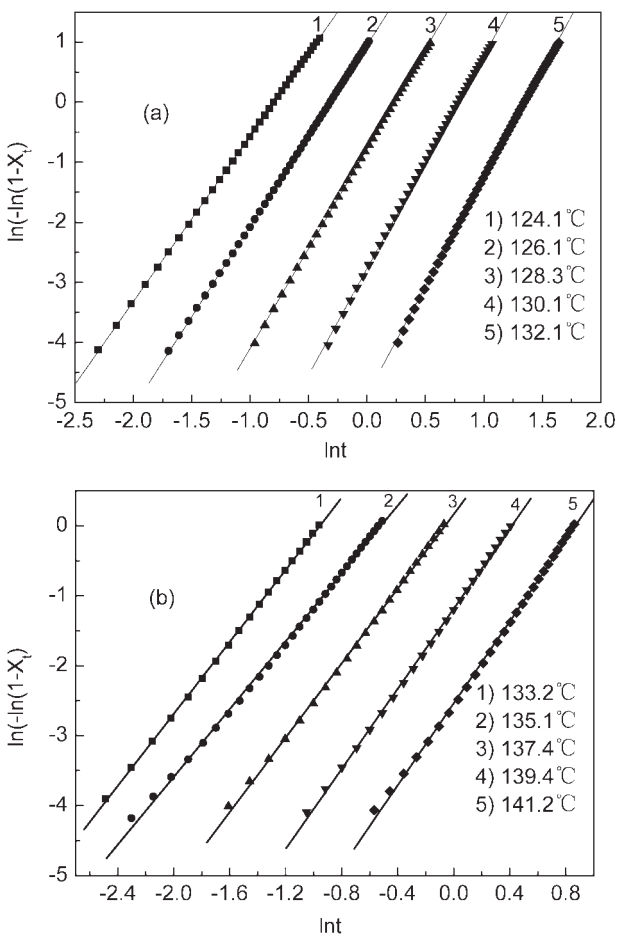

Figure 3 Plots of $\ln(-\ln(1-X_t))$ versus lnt for isothermal crystallization of (a) iPP and (b) iPP/BCHE11.

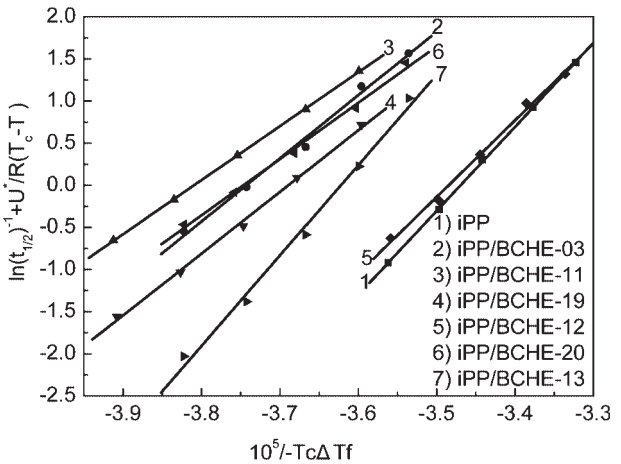

Figure 4 Plots of $\ln(t_{1/2})^{-1}+\frac{U^*}{R(T_c-T_\infty)}$ versus $1/(-T_c\Delta Tf)$ for iPP and nucleated iPP.

where, b_0 is the thickness of the surface layer, defined by the crystalline lattice parameter. σ and σ_e are interfacial free energies per unit area parallel and perpendicular to the molecular chain direction, respectively. k is the Boltzman constant and ΔH is the theoretical heat of fusion. The value of σ can be obtained from the following expression:

$$\sigma = ab_0\Delta H \tag{13}$$

where, a is a numerical constant and equal to 0.1, b_0 is 6.56×10^{-10} m, and ΔH is 1.34×10^8 J/m^3 for iPP, then the value of σ for iPP is 8.79×10^{-3} J/m^2, so the fold surface free energy (σ_e) can be directly obtained from K_g and the results are also listed in Table I. It can be seen that the values of K_g and σ_e of iPP decrease with the addition of nucleating agents. Since, the surface nucleation barrier is positive proportion to K_g,[25] the decrease of K_g indicates that the addition of nucleating agents will lead to the increase of surface nucleation rate. The fold surface free energy of polymers reflects the magnitude of work to bend the polymer chain back upon itself so that it can re-enter the crystal in a manner consistent with the lattice structure.[25] Its value depends on the undercooling or crystallization regime, and meanwhile also related to the composition and microstructure of polymers. The decrease of σ_e nucleated iPP means the decrease of the fold surface free energy of iPP segment, which favor regular folding of the molecule chain, i.e., crystal growth. Therefore, nucleating agents accelerate not only surface nucleation rate but also growth rate of crystal. However, it is noticed that different nucleating agents show different effect to decrease σ_e and the trend is almost consistent with that obtained from the Avrami equation. The difference can be reasonably explained by recalling the already mentioned crystal lattice matching between the nucleating agents and iPP.

Nonisothermal crystallization

Practical processes are usually carried out under nonisothermal crystallization conditions. To search for the optimum conditions in an industrial process and to obtain products with better properties, it is necessary to have quantitative evaluations on the nonisothermal crystallization process, so the study of nonisothermal crystallization kinetics is of great practical importance. The nonisothermal crystallization of iPP and nucleated iPP were carried out by DSC with the cooling rates of 5, 10, 20, 30, and 40°C/min. The thermograms of virgin iPP and iPP/BCHE11 are showed in Figure 5. Those of iPP nucleated with other nucleating agents are similar with that of iPP/BCHE11. With the increasing of cooling rate, crystallization peak temperature of iPP (T_{cp}) shifts to lower temperature. With the addition of bicyclo[2.2.1]heptene dicarboxylate salts, T_{cp} of iPP increased greatly except BCHE12. When the cooling rate is 10°C/min, T_{cp} of iPP/HPNE11 is increased from 121.7°C (virgin iPP) to 132.2°C. However, magnesium salt of bicyclo[2.2.1]heptene dicarboxylate (BCHE12) have little effect on T_{cp} of iPP.

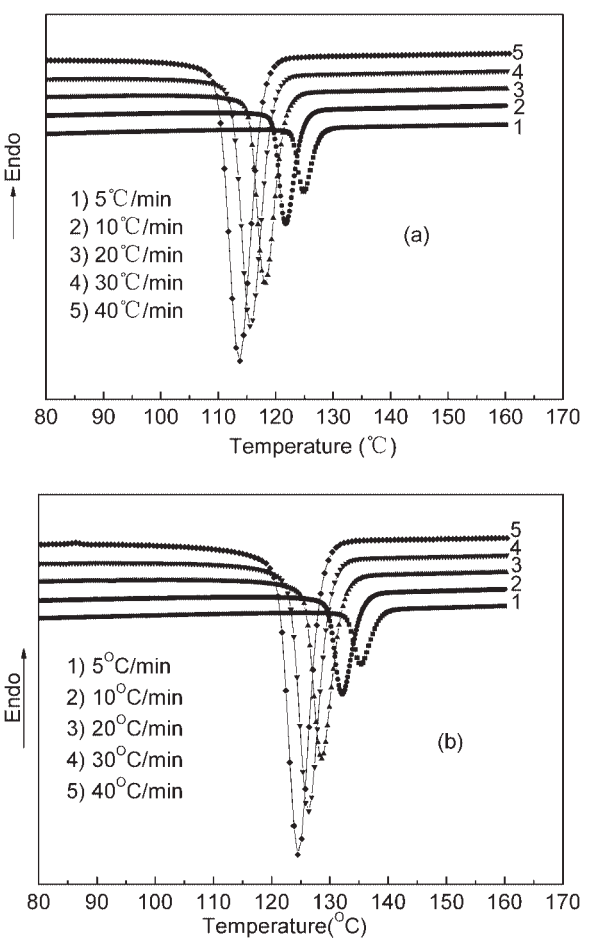

Figure 5 DSC cooling curves of (a) iPP and (b) iPP/BCHE11.

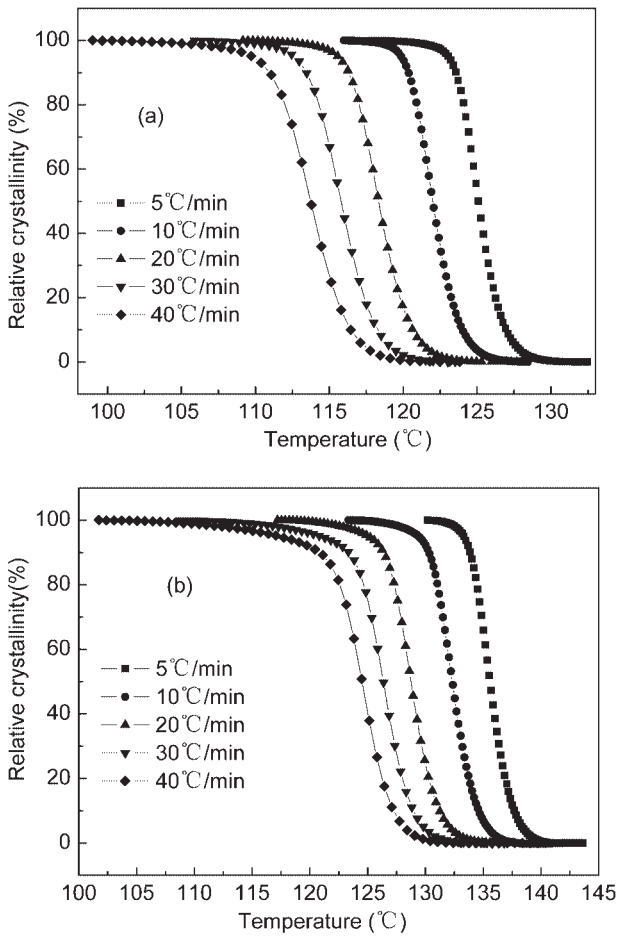

Figure 6 Relative crystallinity of (a) virgin iPP and (b) iPP/BCHE11 at different cooling rates.

By means of integrating the partial areas of the DSC exothermic peaks, the values of the crystalline weight fraction X_w (T) (Fig. 6) can be obtained.

Crystallization half-time $(t_{1/2})$ can be obtained from Figure 6 by equation $t = (T_0 - T)/\Phi$ (where, t is crystallization time, T_0 is onset crystallization temperature, T is crystallization temperature, and φ is cooling rate). The results are listed in Table II. It can be seen that the $t_{1/2}$ decrease by increasing the cooling rates for pure iPP and nucleated iPP, which is in agreement with the polymer crystallization theory.[26] However, the addition of the nucleating agents does not obviously shorten $t_{1/2}$ of iPP, although the crystallization peak temperature is increased.

Now X_w (T) can be converted into X_v (T) by eq. (14):[23]

$$X_v(T) = \frac{X_w(T)\frac{\rho_a}{\rho_c}}{1 - (1 - \rho_a/\rho_c)X_w(T)} \tag{14}$$

where, ρ_a and ρ_c are the bulk densities of the polymer in the amorphous and pure crystalline states, respectively. For iPP, the density of the amorphous phase (ρ_a) is 0.852, and that of the crystallized phase (ρ_c) is 0.935. Therefore, plots of $\ln[-\ln(1 - X_v(T))]$ versus T are showed in Figure 7 and there is good linear relationship in the initial crystallization stage. The values of a and $-aT_q$ can be determined from the slope and intercept of each straight line, and the results are also listed in Table II.

Straight lines can be obtained from plots of obtained T_q versus $\ln \Phi/a$ under different cooling rates (Fig. 8), and good linearity of those curves suggests that the Caze model works well in describing the nonisothermal crystallization for iPP and nucleated iPP. Avrami exponents of iPP and nucleated iPP can be determined from the slope of each straight line and the results are also listed in Table II.

From the results presented in Table II, it is evident that crystallization peak temperature obtained from the experimental data is in agreement with that from Caze method, indicating the validity of Caze method. The crystallization peak temperatures of nucleated iPP are higher than those of pure iPP for the same cooling rate which reveals that nucleating agents act as nucleation sites and accelerate the crystallization of iPP. As for pure iPP, the Avrami exponent is 3.75, corresponding to three-dimensional spherical growth and thermal nucleation in the primary crystallization stage. However, Avrami exponents of nucleated iPP are slightly influenced by adding the nucleating agents except BCHE11 which is proved to be the most effective nucleating agent. Many researchers[27–31] have also observed that the addition of nucleating agents or additives does not diminish the Avrami exponent. Considering the Avrami exponent is mainly influenced by molecular weight, nucleation type, growth geometry, and secondary crystallization, the result attributes to the complicated influence of nucleating agents on nucleation and growth in the crystallization process and too much simplified crystallization kinetics model. It may result in multidimensional crystal due to the different shape of nucleating agents. In addition, the temperature dependence of nucleating efficiency of nucleating agents may result to the competition of homogeneous nucleation and heterogeneous nucleation for special temperature range. However, many models describing the nonisothermal crystallization kinetics do not consider these factors, which would result in some error. Therefore, it needs to develop more perfect mathematical model fitting nonisothermal crystallization kinetics process of nucleated iPP. Meanwhile, it is noticed that the Avrami exponents obtained form the nonisothermal crystallization is not in agreement with those obtained from the isothermal crystallization. This is mainly because they come from the different models. Furthermore, the differences of crystallization behavior in the process

TABLE II
Nonisothermal Crystallization Kinetics Parameters for iPP and Nucleated Ipp

Sample	Φ (°C/min)	T_p[a] (°C)	a	T_q[b] (°C)	$t_{1/2}$ (s)	n	$-\Delta E$ (kJ/mol)
iPP	5	124.8	−1.15	124.9	66	3.75 ± 0.18	249
	10	121.7	−1.12	121.9	34		
	20	118.3	−1.00	118.3	19		
	30	115.5	−0.92	115.7	13		
	40	113.8	−0.83	113.6	12		
iPP/BCHE03	5	133.9	−0.86	133.7	74	3.85 ± 0.08	248
	10	130.2	−0.84	130.1	36		
	20	126.6	−0.81	126.2	19		
	30	123.9	−0.78	123.7	14		
	40	122.5	−0.74	121.7	11		
iPP/BCHE11	5	135.4	−0.96	135.2	60	3.19 ± 0.10	265
	10	132.2	−0.89	131.9	31		
	20	128.6	−0.81	128.2	20		
	30	126.4	−0.76	125.8	15		
	40	124.5	−0.70	123.8	11		
iPP/BCHE19	5	132.9	−0.89	132.6	73	3.74 ± 0.10	246
	10	129.37	−0.88	129.1	35		
	20	125.61	−0.82	125.3	19		
	30	123.37	−0.77	122.8	14		
	40	121.15	−0.75	120.8	11		
iPP/BCHE12	5	125.4	−1.18	125.3	57	3.64 ± 0.12	264
	10	122.4	−1.07	122.2	34		
	20	118.9	−0.97	118.6	17		
	30	116.5	−0.91	116.3	13		
	40	115.1	−0.84	114.4	10		
iPP/BCHE20	5	132.9	−0.98	132.7	65	3.50 ± 0.02	308
	10	130.0	−0.93	129.8	35		
	20	127.0	−0.87	126.4	18		
	30	124.9	−0.84	124.3	13		
	40	123.8	−0.83	122.9	9		
iPP/BCHE13	5	130.3	−1.45	130.1	43	3.71 ± 0.13	337
	10	127.7	−1.36	127.5	24		
	20	125.0	−1.22	124.7	13		
	30	123.4	−1.13	122.7	9		
	40	121.8	−1.04	121.0	7		

[a] Determined from Figure 5.
[b] Calculated from Caze method.

of isothermal and nonisothermal crystallization may contribute to the result. The isothermal crystallization processes under a constant temperature and it is mainly affected by the crystallization temperature, whereas the nonisothermal crystallization does under a changed temperature and it is affected by the cooling rate.

Considering the influence of various cooling rates on nonisothermal crystallization process, Kissinger[32] proposed that the activation energy (ΔE) could be determined by calculating the variation of the crystallization peak with cooling rate.

$$d(\ln(\Phi/T_p^2))/d(1/T_p) = -\Delta E/R \quad (15)$$

where, Φ is cooling rate, T_p is the crystallization peak temperature, and R is the universal gas constant, ΔE is the activation energy of crystallization. The crystallization activation energy was calculated from the slope of $\ln(\Phi/T_p^2)$ versus $1/T_p$ (Fig. 9) line. The results are listed in Table II.

It appears that the absolute values of ΔE for iPP nucleated with bicyclo[2.2.1]hept-5-ene-2,3-dicarboxylate salts are almost higher than that of pure iPP, indicating that the presence of the nucleating agents baffled the transfer of macromolecular segments from iPP melt to the crystal growth surface. We believe that this behavior is a result of interaction between the nucleating agents and polypropylene segments. A similar behavior was reported by Qiang et al.[33] in their study on glass-bead-filled polypropylene. In his article, the addition of glass beads leads to the increase of ΔE because of the weak attraction between the filler and polymer segments.

On the other hand, the observation that T_p of all nucleated iPP is higher than that of pure iPP suggests that BCHED do act as nucleating agents and accelerate the crystallization. However, ΔE of

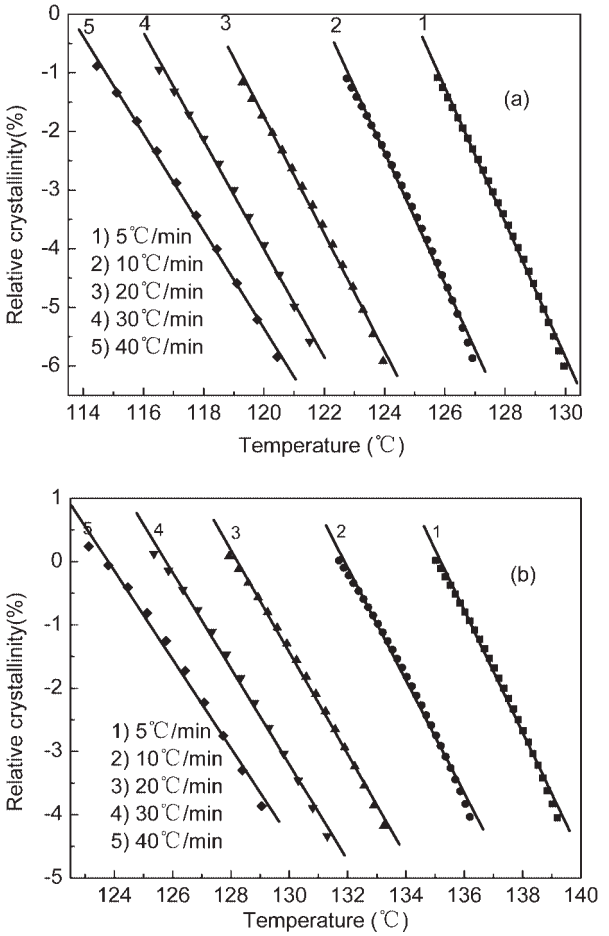

Figure 7 Plots of $\ln[-\ln(1 - X_v(T))]$ versus T for (a) virgin iPP and (b) iPP/BCHE11.

nucleated iPP is higher and is contrary to the expectations of T_p data. It can be interpreted that crystallization process is consisted of nucleation and growth and nucleation rate plays a control role. Although addition of nucleating agents increases the crystallization activation energy of iPP, total crystallization rate is still increased because nucleation rate is accelerated greatly due to the existence of large amounts of heterogeneous nuclei.

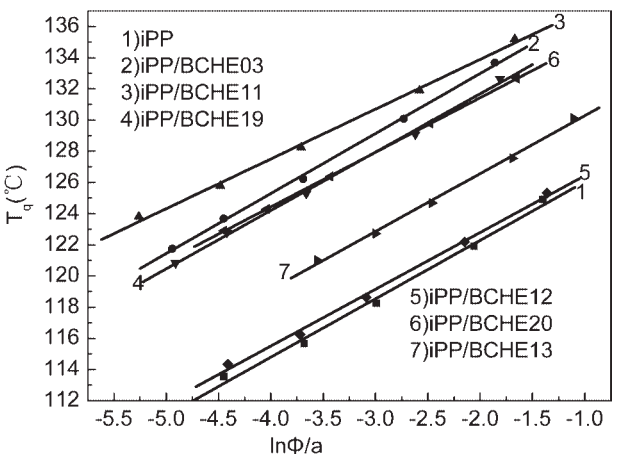

Figure 8 Plots of T_q versus ln Φ/a for iPP and nucleated iPP.

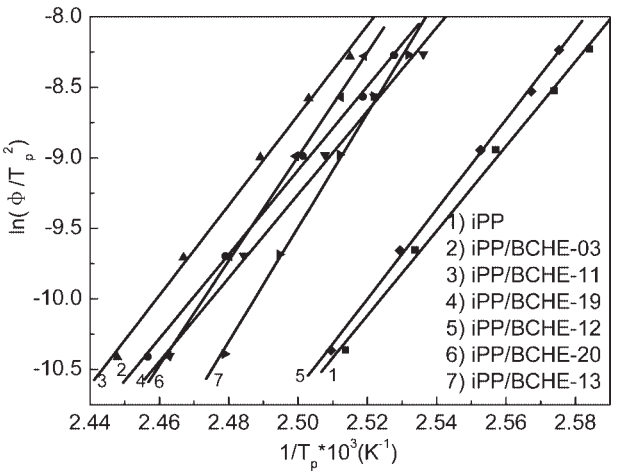

Figure 9 Kissinger plots for calculating the nonisothermal crystallization activation energies for PP and nucleated iPP.

CONCLUSIONS

The isothermal and nonisothermal crystallization kinetics of iPP nucleated with bicycle[2.2.1]heptene dicarboxylate salts (BCHED) have been investigated by Avrami method and Caze method, respectively. Under isothermal condition, the Avrami equation is successfully employed to deal with the crystallization kinetics. The results indicate the nucleating agents BCHED obviously shorten the crystallization time of iPP and nucleation model is heterogeneous nucleation. The interfacial free energy per unit area perpendicular to PP chains σ_e values of iPP were calculated by Hoffman theory. The results show that the nucleating agents favor the crystal growth of iPP. Difference of nucleation effect of different nucleating agents can be reasonably explained by the degree of crystal lattice matching between the nucleating agents and iPP. Under nonisothermal condition, the Caze method is employed to deal with the crystallization kinetics of iPP and nucleated iPP. The results indicate the nucleating agents accelerate the crystallization of iPP. The result is consistent with that obtained from the isothermal crystallization process. Compared with pure iPP, the Avrami exponents of nucleated iPP change little in the nonisothermal crystallization process. The crystallization active energy was determined by Kissinger method. The results show that the interaction between molecule chain of nucleating agents and that of iPP will hinder transfer of macromolecular segments of iPP.

References

1. Mandelkern, L. In Comprehensive Polymer Science: The Synthesis, Characterization, and Applications of Polymers; Allen, G.; Bevington, J., Eds.; Pergamon Press: New York, 1989; Vol. 2: Polymer Properties.
2. Jin, Y.; Hiltner, A.; Baer, E. J Polym Sci Part B: Polym Phys 2007, 45, 1788.
3. Kristiansen, M.; Werner, M.; Tervoort, T.; Smith, P. Macromolecules 2003, 36, 5150.
4. Marco, C.; Ellis, G.; GÓmez, M. A.; Arribas, J. M. J Appl Polym Sci 2002, 84, 2440.
5. Zhang, G. P.; Yu, J. Y.; Xin, Z.; Gui, Q. D.; Wang, S. Y. J Macromol Sci Phys 2003, B42, 663.
6. Zhang, Y.-F.; Xin, Z. J Appl Polym Sci 2006, 101, 3307.
7. Mai, K. C.; Wang, K. F.; Han, Z. W.; Zeng, H. M. J Appl Polym Sci 2001, 81, 78.
8. Yoshimoto, S.; Ueda, T.; Yamanaka, K.; Kawaguchi, A.; Tobita, E.; Haruna, T. Polymer 2001, 42, 9627.
9. Akio, S.; Hirokazu, N. Eur. Pat. 280,297 (1988).
10. Eisuke, S.; Koichi, Y. Jpn. Pat. 2,003,306,586 (2003).
11. Tobita, E.; Urushibara, T.; Shimizu, T.; Kawamoto, N.; Jpn. Pat. 2,003,335,968 (2003).
12. Jang, G. S.; Cho, W. J.; Ha, C. S. J Polym Sci B: Polym Phys 2001, 39, 1001.
13. Li, C. C.; Zhu, G.; Li, Z. Y. J Appl Polym Sci 2002, 83, 1069.
14. Jin, Y.; Hiltner, A.; Baer, E. J Appl Polym Sci 2007, 105, 3260.
15. Stephen, E.; Chantelle; Kent, E.; Markus, A. W. O. 98/29494 (1998).
16. Hoffman, J. D. Polymer 1983, 24, 3.
17. Caze, C.; Devaux, E.; Crespy, A.; Cavrot, J. P. Polymer 1997, 38, 497.
18. Jeziorny, A. Polymer 1978, 19, 1142.
19. Ozawa, T. Polymer 1971, 12, 150.
20. Liu, T. X.; Mo, Z. S.; Wang, S. E.; Zhang, H. F. Polymer Eng Sci 1997, 37, 568.
21. Kissinger, H. E. J Res Natl Inst Stand 1956, 49, 7.
22. Avrami, M. J Chem Phys 1939, 7, 1183.
23. Avrami, M. J Chem Phys 1940, 8, 212.
24. Kim, P. C.; Gan, S. N.; Chee, K. K. Polymer 1999, 40, 253.
25. Hoffman, J. D.; Davis, G. T.; Lauritzen, J. I., Jr. In: Treatise on Solid State Chemistry; Hannay, N. B., Ed.; Plenum Press: New York, 1976; Vol. 3, Chapter 7.
26. Mandelkern, L. Crystallization of Polymers; McGraw-Hill: New York, 1964.
27. Rybnikar, F. J Appl Polym Sci 1982, 27, 1479.
28. Kowalewski, T.; Galeski, A. J Appl Polym Sci 1986, 32, 2919.
29. Avella, M.; Martuscelli, E.; Sellitti, C.; Garagnani, E. J Mater Sci 1987, 22, 3185.
30. Tai, H. J.; Chiu, W. Y.; Chen, L. W.; Chu, L. H. J Appl Polym Sci 1991, 42, 3111.
31. Kim, C. Y.; Kim, Y. C.; Kim, S. C. Polym Eng Sci 1993, 33, 1445.
32. Kissinger, H. E. J Res Natl Bur Stand 1956, 57, 217.
33. Qiang, Y.; Jiang, W.; An, L. J.; Misra, R. D. K. J Appl Polym Sci 2006, 102, 2026.